

Identification of hydrometeors and other targets by dual-polarization radar

Martin P. M. Hall, John W. F. Goddard, and Stephen M. Cherry

Rutherford Appleton Laboratory

(Received October 18, 1982; revised March 30, 1983; accepted May 18, 1983.)

Whereas different hydrometeor types cannot be readily distinguished using radar reflectivity alone, this paper shows how the differential reflectivity available from dual-polarization radars can be used as an indicator of hydrometeor type (when supported by reflectivity factor also), and that the spatial variability of differential reflectivity is a useful addition. Various hydrometeor types, ground targets, and burnt chaff from straw fires may be identified, whereas conventional radar reflectivity measurement alone would require considerable pattern recognition to make the same distinctions.

1. INTRODUCTION

The principle of dual-polarization radar is to measure Z_H and Z_V , the effective radar reflectivity factors for horizontally and vertically polarized radar transmissions, respectively, and to then compute the differential reflectivity Z_{DR} , which, when expressed in decibels, is defined by

$$Z_{DR} = 10 \log_{10} (Z_H/Z_V) \quad (1)$$

Because raindrops are oblate to a degree that depends upon their size, Z_H is greater than Z_V , when observing at low elevation angles, and so Z_{DR} in rain is positive by an amount depending on the median drop size.

Probably the most important use of the measurement of Z_{DR} to date has been to improve the accuracy of remotely measuring rainfall rates and specific attenuation due to rain. This has been discussed in some detail elsewhere [Seliga *et al.*, 1981a; Goddard and Cherry, this issue; Cherry *et al.*, 1981]. However, the distinction of rainfall from other targets can be equally important, and Hall *et al.* [1980b] and Seliga *et al.* [1981b] have given some indication of how dual-polarization radars may be used to distinguish rain from ice particles. This capability very much extends the value of such radars in many applications, for example, in examining the effect of rain and other hydrometeors on the attenuation of radio waves on earth-space paths, where rain and ice have quite different effects [Cherry *et al.*, 1981]. However, priorities in previous work have not included a sys-

tematic examination of different hydrometeor types and other target types. In particular, it is to be expected that recognition of regions of different ice forms may help in modeling the effects that such ice regions have in reducing cross-polar isolation on earth-space radio paths where dual-polarization is employed for frequency reuse. Also, it is felt that dual-polarization radar data have great potential for cloud physics studies.

The prime objective of the study outlined in this paper was to determine the extent to which the additional data provided by dual-polarization radar (compared with those data available from conventional radar) can be used to distinguish hydrometeor types and to distinguish hydrometeors from other targets such as ground echoes, smoke plumes, etc. Toward this objective, an analysis has been made of the range of values of Z_H (generally referred to below as Z) and Z_{DR} . Whereas Z depends on the number and size of hydrometeors, as well as their shape and refractive index (both of which are a function of hydrometeor type), Z_{DR} depends only on the shape and refractive index (assuming Rayleigh scattering). From Battan [1973] it may be seen how a small ratio a/b produces a large Z_{DR} for water (of dielectric constant near 80), whereas it produces a much smaller Z_{DR} for ice (of dielectric constant near 3). Here a and b are the minor and major axes of an oblate spherical particle. The ratio of the scattering cross sections, σ_H/σ_V , for horizontal and vertical polarizations is illustrated in Figure 1, where the density of the ice/air mixture is indicated. This point will be seen to be of major significance when considering the data examples of section 3. In addition to Z_{DR} , its spatial variability (described below) is a good indication of

Copyright 1984 by the American Geophysical Union.

Paper number 3S0824.
0048-6604/84/003S-0824\$08.00

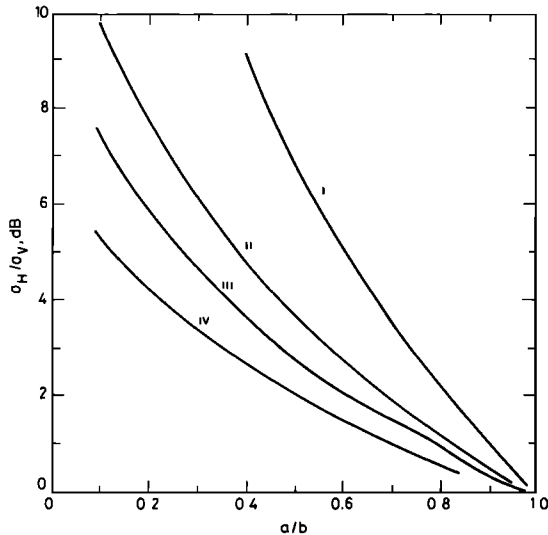


Fig. 1. Ratio of scattering cross sections for horizontal and vertical polarizations as a function of minor-to-major axis ratio of an oblate spheroid for water (curve i), solid ice of 0.92 g cm^{-3} (curve ii), an ice-air mixture of 0.5 g cm^{-3} (curve iii), and an ice-air mixture of 0.1 g cm^{-3} (curve iv).

target type in certain cases, and this variability has been given special attention.

2. DATA COLLECTION

The radar used for the present study has been fairly fully described by *Hall et al.* [1980a] and *Cherry and Goddard* [1982]. Situated at Chilbolton in southern England, it has a 25-m diameter antenna giving a 0.25° beam width (one-way to -3 dB points) at the operating frequency of 3076.5 MHz. Alternate pulses are transmitted (and received) on horizontal and vertical polarizations. Digitization of received power prior to averaging is in 256 steps of 0.25 dB (i.e., 64 dB range). Each range-gated data sample comprises a spatial average (linear power) over 300 m (four pulse volumes). Time averaging (linear power) for each data sample is over 210 ms every 240 ms (i.e., 64 transmitted pulses on each polarization). The worst case systematic errors in measuring Z and Z_{DR} were estimated to be ± 0.7 dB and ± 0.1 dB, respectively, while the standard deviations of the random errors when measuring rain echoes were also estimated to be 0.7 dB and 0.1 dB, respectively. A detailed study of the accuracy of measurement has been given by *Cherry and Goddard* [1982].

To investigate, quantitatively, the extent to which the spatial variability of Z_{DR} is a good indicator of target type, data were normally taken from inclined

planes, typically elevated at 1° to 2° , from 30 selected range gates (each an average over 300 m) while the radar beam moved over (typically) 30 beam widths (each sample covering 0.25°). Within these 900 samples, a study was made of Z and Z_{DR} , and of the corresponding standard deviations S_Z and S_{DR} . Here S_Z and S_{DR} were computed from measurements of the differences of adjacent azimuth samples for a given range gate. By this means any trend in Z or Z_{DR} is not mirrored in the values of S_Z or S_{DR} . The spread of S_Z and S_{DR} values quoted was then that evaluated for different ranges.

Estimates of S_Z and S_{DR} obtained from the radar have minimum values limited by the sampling process of the "noisy" signal produced from randomly distributed targets (e.g., hydrometeors) within the pulse volume. Consequently, values of S_Z less than 1 dB or S_{DR} less than 0.2 dB cannot reliably be associated with true spatial variability, and indeed for hydrometeors or other targets where there is a wide variety of shapes and sizes (compared with rain), the limit to S_{DR} may be much larger [*Cherry and Goddard*, 1982].

3. RAIN AND OTHER HYDROMETEOR TARGETS

Before considering specific examples, it is useful to note some general statements about Z_{DR} of ice particles that have resulted from earlier studies by the authors. The discussion of Figure 1 is relevant here. Dry snowflakes above the bright band have relatively low Z compared with rain. The low refractive index of snow, which is a low-density ice/air mixture, means that Z_{DR} is always very low, 0.5 dB or less. By contrast, high-density ice hydrometeors (greater than about 0.3 g cm^{-3}) can be very variable in shape and may vary in size from small ice crystals through to hailstones several centimeters across. If such ice particles approximate to spheres, or are nonspherical but tumble so that there is no preferred orientation, they are likely to produce Z up to 50 dBZ (units are decibels, $Z > 1 \text{ mm}^6 \text{ m}^{-3}$), but Z_{DR} less than 0.1 dB. However, relatively high Z_{DR} (up to about 5 dB) may be caused by high-density ice particles with relatively large horizontal dimensions. When particles of solid ice melt to each form waterdrops, Z increases by 6.7 dB. As snowflakes melt to become raindrops, fall speeds increase by a factor of about 4, and so Z reduces by 6 dB from this cause alone. In the examples that follow, these general statements about Z and Z_{DR} help to distinguish hydrometeor types.

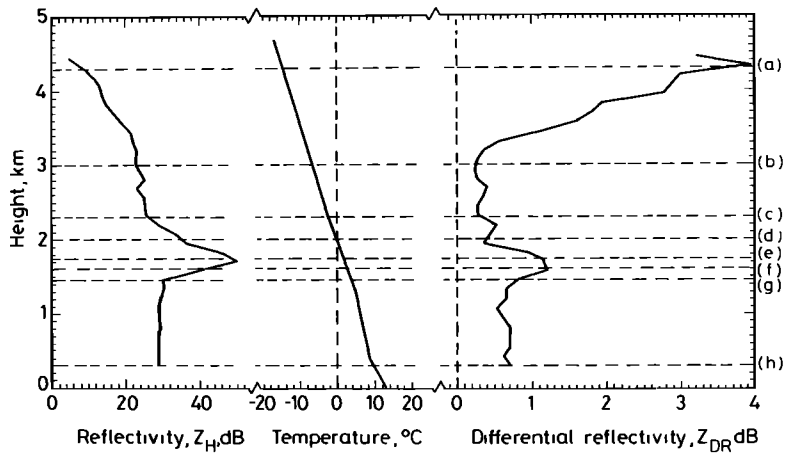


Fig. 2. Variation of Z and Z_{DR} with height, from the vertical section in Plate 1, at 33 km range. Also shown is a temperature profile from a radiosonde ascent at Crawley, 88 km east of Chilbolton, at 1200 UT.

Plate 1 shows a vertical section through the most intense region of a widespread rain cell. There is a pronounced (reflectivity) bright band at all ranges, with values reaching 50 dBZ at 33 km range. Other cuts through the rain cell showed that the bright-band (i.e., region of high Z , but not necessarily high Z_{DR}) melting layer around the periphery is 1.9 km high with rainfall rates below 1 mm h^{-1} , while toward the center of the cell the bright band drops to 1.7 km, and rainfall rates reach 6 mm h^{-1} . These and subsequent values of rainfall rate are computed from Z and Z_{DR} as described by *Goddard and Cherry* [this issue]. In the melting layer above the weaker rain (at less than 28 km range) the largest values of Z and Z_{DR} occur at the same height, while above the more intense rain the peak in Z_{DR} is 100–200 m below the peak in Z (bright band). Generally, the highest values of Z are accompanied by low values of Z_{DR} , and vice versa. Another marked feature in Plate 1 is a region containing high values of Z_{DR} at the top of the detectable cloud, where the reflectivity is less than 10 dBZ.

A likely explanation of these effects may be offered by reference to Figure 2, which shows values of Z and Z_{DR} from Plate 1 at 33 km range, together with radiosonde temperature values, as a function of height. The data have been averaged over three range gates (900 m) to reduce fluctuations due to sampling errors and natural small-scale variations. The various height regions (a to h) can be considered in terms of physical processes as follows:

Region a. Z_{DR} has a maximum value of 4 dB, and Z is between 5 and 15 dBZ, implying highly asym-

metrical crystals (needles or plates) of solid ice, with the large dimensions highly aligned to the horizontal.

Region a–b. Z increases by 16 dB, suggesting crystal growth by riming or accretion. At the same time, Z_{DR} decreases to 0.3 dB, suggesting a combination of loss of a preferred orientation (due to shape changes or the onset of tumbling) and a decrease in particle dielectric constant due to a density decrease.

Region b–c. Z increases slightly, suggesting a little further growth, without an appreciable change in Z_{DR} .

Region c–d. Z now increases more rapidly, by 8 dB in 300 m, probably because of aggregation into large snowflakes, as is to be expected where the temperature is above -5°C .

Region d–e. Both Z and Z_{DR} increase, because of the increased dielectric constant of the now water-coated ice particles. Evidently, the particles will have had some degree of preferred horizontal orientation in the region above, which was not apparent because of the low density (and dielectric constant) of the ice. However, this orientation is made clear once the particles become water coated.

Region e–f. Z decreases by 9 dB; the smaller snowflakes have now melted completely, and their fall speeds have increased to values appropriate for raindrops, causing a decrease in number density and a decrease in reflectivity. By contrast, Z_{DR} is still large, probably because the remaining partially melted large particles have small ice cores to maintain a relatively large oblate shape. At other ranges the difference in height of the peak values of Z and Z_{DR} is even more pronounced.

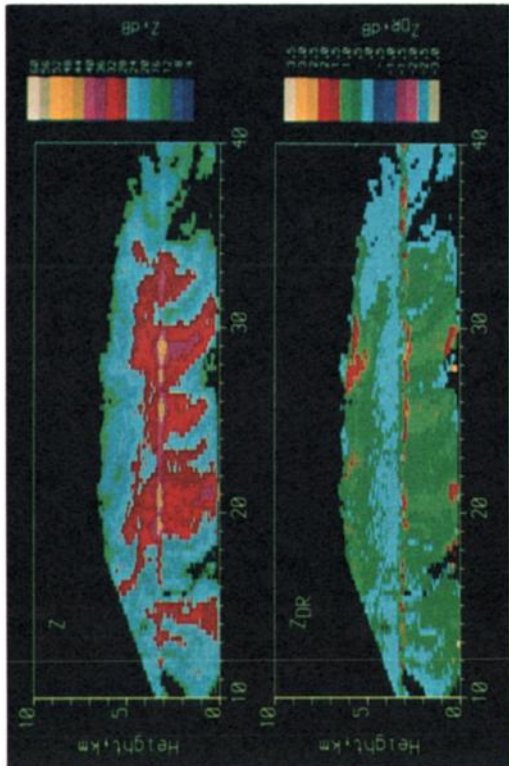


Plate 2. July 25, 1980, at 2306 UT.

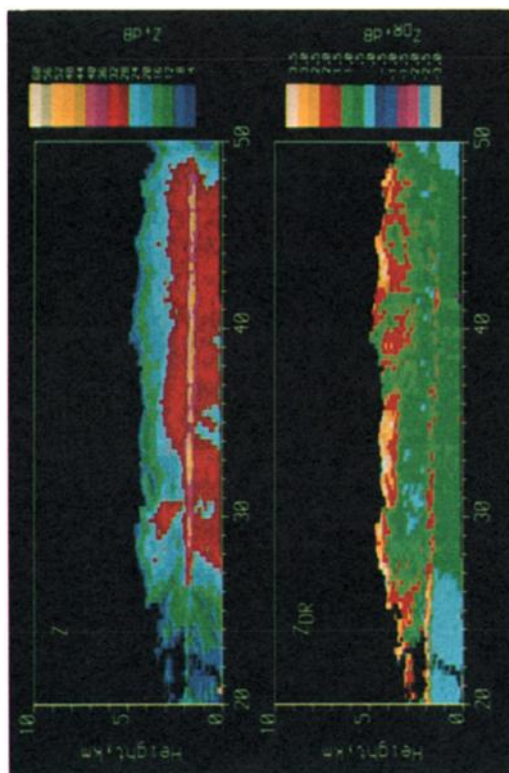


Plate 1. May 21, 1980, at 1358 UT.

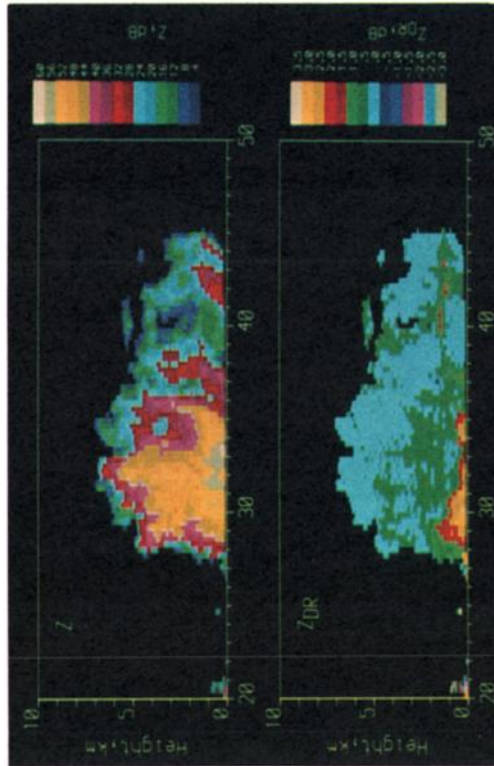


Plate 4. As Plate 3, but displaced by 5° in azimuth.

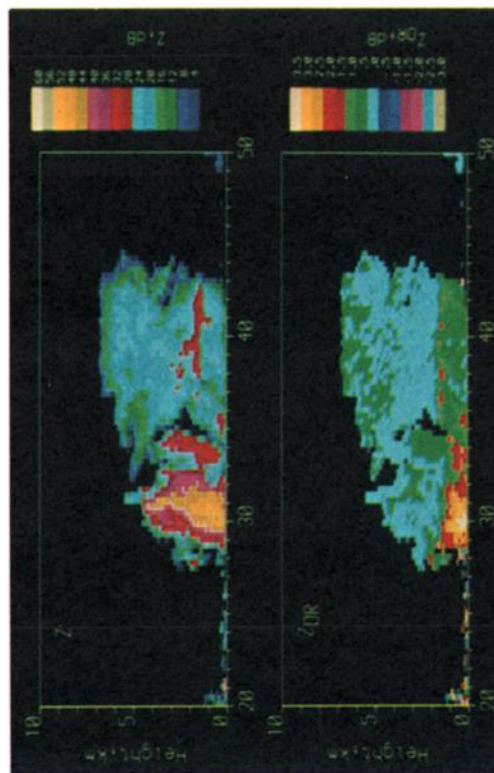


Plate 3. May 20, 1980, at 1502 UT.

Plates 1-4. Vertical sections through rain and ice obtained with dual-polarization radar (note common scale). The horizontal scale is distance, in kilometers.

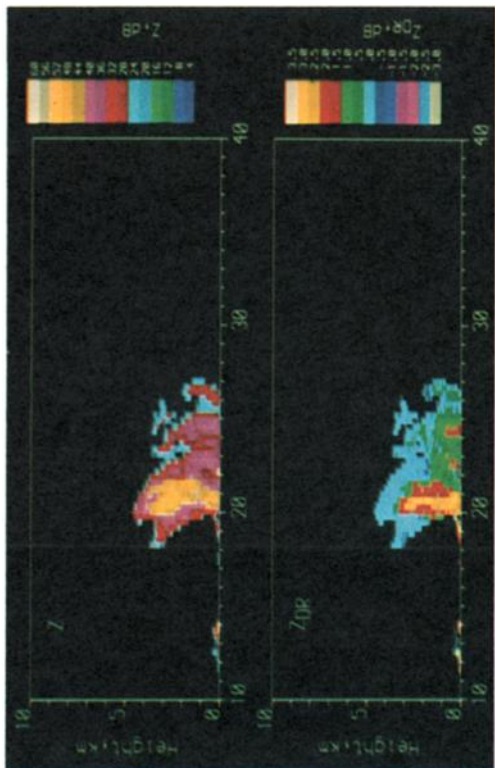


Plate 5. Vertical section through rain and ice obtained on July 2, 1980, at 1635 UT. The horizontal scale is distance, in kilometers.

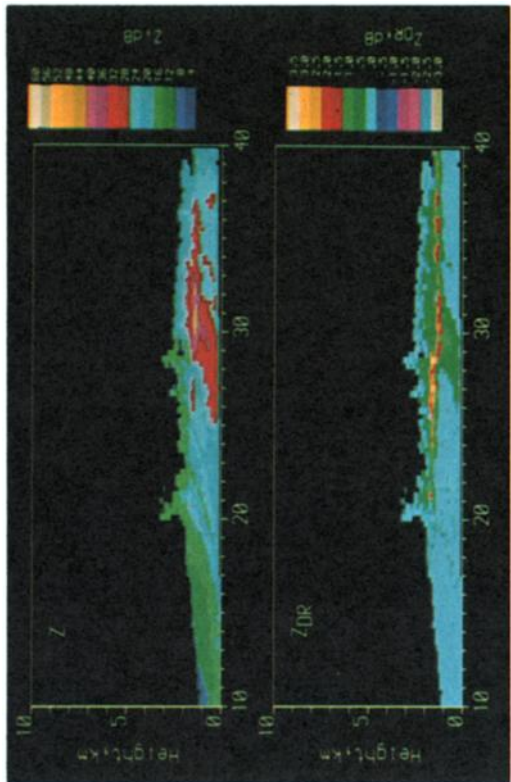


Plate 6. As Plate 5, but for October 28, 1981, at 1619 UT.

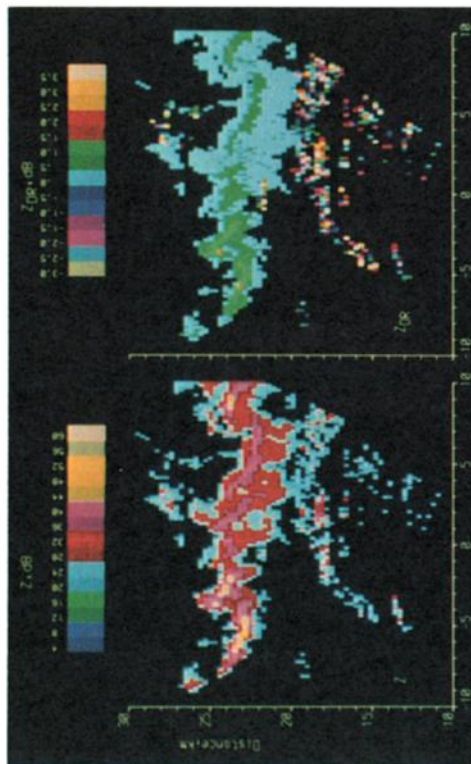


Plate 7. An inclined plane (at 1.5° elevation) containing rain and ground echoes, on July 4, 1980, at 1431 UT. The vertical scale is distance from radar, and the horizontal scale is lateral distance, both in kilometers.

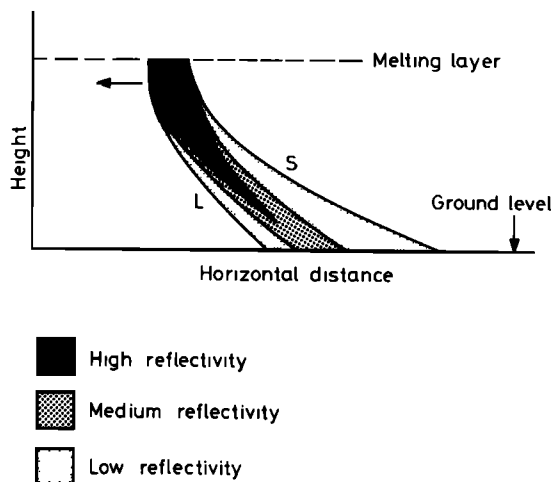


Fig. 3. Stylized representation of moving rain cell, with wind velocity (right to left) increasing with height.

Region f-g. Both Z and Z_{DR} are now decreasing, as even the largest particles complete their melting process. Drop breakup may also be occurring.

Region g-h. No further significant changes in Z or Z_{DR} occur in the rain, which has an intensity of 2.5 mm h^{-1} . (Below 200 m, data are contaminated because of screening by hills.)

While the characteristics of this height profile prevail throughout the rain cell, there are some differences in detail. For example, at ranges less than 28 km the peak values of Z and Z_{DR} in the melting region are coincident in height, and the peak Z_{DR} value is larger, for example, 3.5 dB at 26 km range. Below the melting layer the low values of Z_{DR} (about 0.1 dB) suggest the presence of only small waterdrops caused by small ice particles. The fact that these particles produce such large Z_{DR} in the melting layer suggests that they are wet asymmetrical needles or plates with a much smaller degree of accretion and aggregation here than at greater ranges. It is also noteworthy that Z_{DR} varies considerably in the melting region, as perhaps do the hydrometeor shapes. Often the peak of Z_{DR} in the melting layer is below the peak of Z [Cherry *et al.*, 1981; Hall *et al.*, 1980a, b], but to have the two at the same height is not unusual. Some studies of the variability of Z_{DR} associated with the melting layer have been made in this and other examples, and the small-scale variability indicated by the values of S_{DR} is typically 3 times greater in this region than in the rain.

Plate 2 shows an example in which rain is localized to a number of cells, with a distinct lean due to wind shear below the melting layer. This is particu-

larly noticeable in the cell at 29 km from the radar. The variation of Z with height and distance is somewhat as shown stylized in Figure 3 (based on work by Gunn and Marshall [1975]) where large drops (L) would be expected to fall faster than the small drops (S). Closer inspection of Plate 2 shows just such a sorting, with a region of high Z_{DR} (due to large drops) within the first 1 km from ground at 29 to 30 km distance. The trailing edge of the cell has much smaller values of Z_{DR} (due to smaller drops). As the cell advances (toward the radar) past a point on the ground, there is a rapid increase in Z at the leading edge and a gradual falloff at the trailing edge.

As with Plate 1, this is an example of (1) high Z_{DR} and low Z well above the melting layer (above 5 km in this case), probably due to high-density highly oriented ice particles, and (2) low Z_{DR} and rising Z within 1 km above the melting layer, probably due to aggregation. Again, at some ranges, high values of Z and Z_{DR} occur in the melting layer at the same height, and at other ranges there is a marked difference in height.

Plate 3 shows an example of a vertical section through rain and ice resulting from a cold frontal system associated with a trough of low pressure over central England. Considering first the more distant rain cell between 37 and 43 km from the radar, there is a clear transition from ice to water at about 1.6 km height, indicated by an enhancement of Z in the melting layer of up to 10 dB, and an increase in Z_{DR} from 0.1 dB in the ice phase (snow) to 1.7 dB during melting before decreasing to approximately 0.5 dB in the rain below. Above about 4 km height, ice with Z_{DR} values of up to 0.5 dB is present, suggesting a change in symmetry and/or particle density between here and the ice, with lower Z_{DR} below. Both ice regions exhibit low values of S_{DR} (~ 0.05 dB) and have S values between 0.9 and 1.7 dB. Below the melting layer the rain is relatively weak, about 2 mm h^{-1} .

The nearer rain cell, with a central core at 31 km range, presents a picture very different from the one at greater range, presumably as a result of the very different process involved. Again there is a transition from ice to water starting at a similar height, but in this case shown only by an increase in Z_{DR} from low values of generally less than 0.5 dB to values of 3 dB or more. There is no clear height zone of Z or Z_{DR} maxima (as at 40 km range), but a distinct increase in both between about 2 km and 1 km height. Below 1 km height, both Z and Z_{DR} are still increasing slowly,

and it is likely that this is because the melting has not been completed by the time the precipitation reaches the ground. The large Z_{DR} is probably caused by large distorted drops of water having an ice core.

The region of moderate Z close to ground between 20 and 29 km, and higher values of Z at 21 to 22 km distance, are due to ground echoes. Z_{DR} is highly variable, both positive and negative. The fact that these appear to occur up to 1.3 km height at 21 km distance is due to the echoes being in the antenna side lobes. This can be somewhat confusing, since such echoes can be absent when the beam is close to horizontal, but appear at a low elevation due to a target off the direction of look. Such ground echoes are considered further in section 4.

Plate 4 shows a second vertical section made 13 s after Plate 3, on a bearing 5° away. Here Z reaches 57 dBZ at 1 km height (distances 31.5 to 34 km) and exceeds 60 dBZ close to ground at 33 to 34 km distance. Evidently, at 33.5 to 34 km distance, melting has barely started as the precipitation reaches the ground. The very marked depression of the melting height is probably due to cooling of the air by the large flux of melting particles in a cell where this has persisted for some time.

Plate 5 shows at range 20 to 21 km a fairly rare example of a vertical section through rain where a narrow column of both high Z and Z_{DR} extends up to 3.5 km height, without any clear change at the melting layer height (found at 2 km in other regions of this cell). The interpretation given to this is that the column is one containing supercooled water carried up in an updraft. Such supercooled water can be a considerable hazard to aircraft (especially helicopters) flying above the melting layer, since the airframes are likely to be below freezing, and the build-up of ice would then be rapid. None of the examples seen on the Chilbolton radar have had horizontal extent greater than about 1 km. Small areas of ice with negative Z_{DR} values (as low as -0.5 dB) can be seen around the top of this column of water. Such negative values are rarely seen at Chilbolton, even in ice. They may be caused by the longer axis of these ice crystals being unusually aligned to the vertical by wind shear or electric fields. Alternatively, these hydrometeors may be conical graupel falling with the longer dimension vertical. This example also shows very marked permanent echoes from ground at ranges 12 to 14.5 km (see section 4).

Plate 6 highlights two interesting features. First, and most obvious, is the very substantial amount of

wind shear causing the rain cells at about 30 km range to lean at about 65° to the vertical, an effect described with reference to Figure 2. A second, less obvious, feature is the presence of rain with very low Z_{DR} values (0.1 dB and less) yet with reflectivity values of 25–30 dBZ. If an exponential drop size distribution is assumed, these values lead to unrealistically high values of rainfall rate (10 mm h^{-1}). Corroborating evidence from ground-based distrometer data [Goddard and Cherry, this issue] shows this is caused by a virtually monodisperse distribution of raindrops of about 1 mm diameter. Because these drops are so small, and falling only slowly, the lean of the cells due to wind shear is increased to 75° from vertical.

4. NONMETEOROLOGICAL ECHOES

The interpretation of meteorological radar data is frequently complicated by the presence of nonmeteorological targets such as ground echoes. Consistent echoes from ground targets can be eliminated by comparison with previously recorded maps when no rain was present, but this cannot be done when the observation of ground echoes is due to anomalous propagation. Moreover, rain may occur in the same area as the ground echoes. Hence a radar which can automatically distinguish meteorological targets from others is particularly useful.

Plate 7 shows plots of Z and Z_{DR} from rain (in the main beam) in the presence of permanent ground echoes (in the side lobes). The data were collected from an inclined plane elevated at 1.5° . The line of maximum rain intensity some 20 to 25 km from the radar (at center of scan) was sampled at a height of about 600 m, whereas range-height indication plots showed that the melting layer height was about 1.2 km. The distinction between rain and ground echoes is most clearly seen from Z_{DR} , the ground echoes occurring at distances less than 18 km, apart from some at 25 to 28 km slightly to the right of scan center. Within a region of rain selected for a special study (between ranges of 21 to 23 km and 5 km wide), Z varied from 15 to 40 dBZ in the rain, while Z_{DR} varied from 0 to 1.2 dB; S_Z was between 1.0 and 3.0 dB, and S_{DR} was less than 0.13 dB; i.e., while S_Z was variable, S_{DR} was only a little larger than expected for spatially uniform rain.

For the region containing ground echoes, the range of values of Z_{DR} is much wider than that for rain, between -4.3 and $+4.6$ dB; indeed, most of the sample volumes show negative Z_{DR} values. Also, the

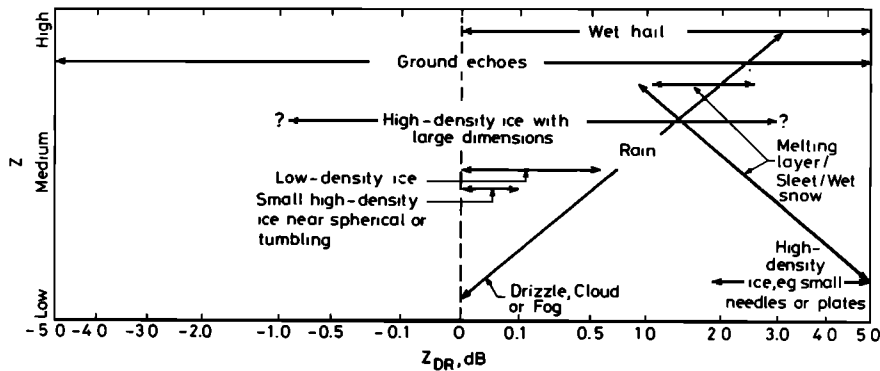


Fig. 4. Expected characteristics of Z and Z_{DR} at 10 cm wavelength for various hydrometeor types (and ground echoes). See comments in text on the double line for melting layer/sleet/wet snow.

apparent small-scale spatial variability for Z_{DR} is large, between 1.5 and 3.5 dB, whereas Z and S_Z are comparable to the values seen for the rain in this example. Although these characteristics are for ground echoes observed in the antenna side lobes, other data where the ground echoes are in the main beam show very similar results. The example of ground echoes shown here is for about 100-km² area of rolling terrain.

Particularly interesting echo characteristics have been positively identified by *Zhang and Cherry* [1983] as originating from the effects of field fires when farmers were burning straw stubble in nearly calm weather conditions. The echoes were consistent with those of weak rain, but Z_{DR} showed this not to be the case, as, although the values were large and positive, they were also very variable spatially. Some such echoes extend to some 4 km in height and have values of Z up to 50 dB, with a nucleus of low Z_{DR} (presumably due to tumbling of the straw chaff), an inner shell (at about 1 km radius) of high Z_{DR} (e.g., 7 dB, presumably as long and thin straw chaff settles), and an outer region of lower Z_{DR} and lower Z (presumably due to smaller straw chaff). The high values of Z were attributed to condensation of water on the chaff.

5. SUMMARY

Although even the small amount of radar data presented in this paper illustrates many meteorological effects, the main points may be summarized by reference to Figure 4. The dual-polarization radar parameter Z_{DR} (and its standard deviation S_{DR}) clearly distinguishes the melting layer and ground echoes from each other, and from regions of precipitation. By contrast, Z is only a support indicator of target type,

since it depends on the number of hydrometeors in the radar pulse volume. Ground echoes have widely ranging Z_{DR} values (mainly negative), and the spatial variability is high. Straw chaff fires have been found to produce echo forms with Z_{DR} readily distinguishable from that of hydrometeors. Rain and ice are less clearly distinguished from each other, and often the distinction can only be made by observing the changes in Z and Z_{DR} at the transition between the phases. Often a variety of hydrometeor types may exist together. However, the following generalizations may be made:

1. Wet hail has high Z values due to the large size, and a wide range of Z_{DR} according to whether it is tumbling or not.

2. Dry high-density ice with large dimensions has a wide range of Z_{DR} (possibly even negative in the case of conical graupel) and medium Z .

3. Low-density ice, or small high-density ice which is near spherical or tumbling, has lower Z and low Z_{DR} (due to the low refractive index in the former case and lack of orientation in the latter).

4. High-density ice with small dimensions, e.g., small needles or plates (which tend to fall with the larger dimension horizontal), has high Z_{DR} , but low Z . These often seem to occur at high levels before riming or aggregation occurs at lower levels.

5. Rain has a wide range of positive Z_{DR} generally correlated with Z . The lower end (i.e., Z_{DR} less than about 0.1 dB) is characteristic of drizzle, cloud, or fog.

6. The melting layer/sleet/wet snow will generally have medium/high values of Z_{DR} . Much depends on what is melting. Large snowflakes when melting will exhibit high Z and high Z_{DR} . Small ice chips when melting will show lower Z , but possibly higher Z_{DR} .

S_{DR} is typically 3 times larger in this region than in the rain below.

The use of Z_{DR} in interpreting developments of hydrometeor types in precipitation cells holds great promise, and such studies should greatly assist progress in many other disciplines where there is a need to know the size, shape, and density of hydrometeor forms in various locations in such a cell.

REFERENCES

- Battan, L. J., *Radar Observations of the Atmosphere*, University of Chicago Press, Chicago, Ill., 1973.
- Cherry, S. M., and J. W. F. Goddard, The design features of dual-polarisation radar which affect the accuracy of measuring differential reflectivity, paper presented at URSI Open Symposium on Multiple-Parameter Radar Measurements of Precipitation, Bournemouth, United Kingdom, 1982.
- Cherry, S. M., J. W. F. Goddard, and M. P. M. Hall, Use of dual-polarisation radar data for evaluation of attenuation on a satellite-to-earth path, *Ann. Telecommun.*, *36*, 33–39, 1981.
- Goddard, J. W. F., and S. M. Cherry, The ability of dual-polarization radar (copolar linear) to predict rainfall rate and microwave attenuation, *Radio Sci.*, this issue.
- Gunn, K. L. S., and J. S. Marshall, The effect of wind shear on falling precipitation, *J. Atmos. Sci.*, *12*, 339–349, 1975.
- Hall, M. P. M., S. M. Cherry, and J. W. F. Goddard, Use of dual-polarisation radar to measure rainfall rates and distinguish rain from ice particles, The Record of the IEEE 1980 International Radar Conference, *Publ. 80CH1493-6 AES*, Inst. of Electr. and Electron. Eng., New York, 1980a.
- Hall, M. P. M., S. M. Cherry, J. W. F. Goddard, and G. R. Kennedy, Raindrop sizes and rainfall rate measured by dual-polarisation radar, *Nature*, *285*, 195–198, 1980b.
- Seliga, T. A., V. N. Bringi, and H. H. Al-Khatib, A preliminary study of comparative measurements of rainfall rate using the differential reflectivity radar technique and a raingage network, *J. Appl. Meteorol.*, *20*, 1362–1368, 1981a.
- Seliga, T. A., J. L. Peterson, and V. N. Bringi, Hydrometeor characteristics in the May 2, 1979 squall line in central Oklahoma as obtained from radar differential reflectivity measurements during SESAME, in *Proceedings 20th Conference on Radar Meteorology*, American Meteorological Society, Boston, Mass., 1981b.
- Zhang, M. G., and S. M. Cherry, Backscatter characteristics of burnt straw particles, paper presented at IEEE/APS Symposium and National Radio Science Meeting, Inst. of Electr. and Electron. Eng., Houston, Tex., 1983.

S. M. Cherry, J. W. F. Goddard, and M. P. M. Hall, Rutherford Appleton Laboratory, Chilton, Didcot, Oxfordshire, OX11 0QX, United Kingdom.